Robust design of a polygonal shaft-hub coupling

R. Citarella, M. Perrella

Department of Industrial Engineering, University of Salerno, via Giovanni Paolo II 132, Fisciano (SA), Italy
rcitarella@unisa.it

ABSTRACT. In this work, the Taguchi method is applied for the optimal choice of design parameter values for a polygonal shaft-hub coupling. The objective is to maximize a performance function, minimizing, at the same time, its sensitivity to noises factors (robust design). The Design of Experiments (DoE) is adopted to set up a plan of numerical experiments, whose different configurations are simulated using the Boundary Element Method (BEM).

KEYWORDS. Robust design; Boundary Element Method; Taguchi method; Polygonal shaft-hub coupling.

INTRODUCTION

In polygonal shaft-hub couplings, the torque transmission takes place thanks to normal and friction forces at the interface between the joined components.

The common features of these couplings include: compact construction, self-alignment, absence of protruding elements that may cause high stress levels, efficient transmission of static-oscillating torques even with small dimensions, easy hub interchangeability (in case of failure) and, for polygonal shapes, such as those with 4 lobes, the possibility of displacement under load [1]. These types of couplings are highly competitive when compared to traditional ones that use keys, fasteners and splined shafts.

Nevertheless, the difficult workability (with steel requiring special grinding machines) and laborious calculation of the stresses, due to the lack of rotation symmetry, along with a tri-axial stress state, discouraged designers and constructors in the past, with them preferring traditional couplings over polygonal ones.

The development of CNC grinding machines, the introduction of sintered materials (allowing for production by moulding), along with the improvement of hardware and software resources, making it possible to carry out accurate assessments for the dimensioning, circumvented those drawbacks, making the use of polygonal couplings very appealing.

The first analysis of the biaxial stress and strain states in the shaft-hub was proposed by Mechnik that used the Finite Element Method (FEM) [2], followed by many literature works up to recent time [3].

The numerical analysis of the coupling by FEM greatly reduced the simplification of the coupling model, with the results becoming reliable, as highlighted by the comparison of the FEM numerical results against the experimental ones obtained from optical methods [4] and against BEM (Boundary Element Method) numerical results [5]. Mechnik's study, along with those that followed [6-7], dealt with shaft-hub couplings with the most commonly used P3G normalized polygonal profiles. Figure 1 shows a normalized profile with 3 lobes, whilst its parametric equation, defined in 1959 by Filemon [8] and valid in general for profiles with n lobes is reported in Eq. (1), where the parameters D_m and e are, respectively, the *diameter* and *eccentricity* of the profile.
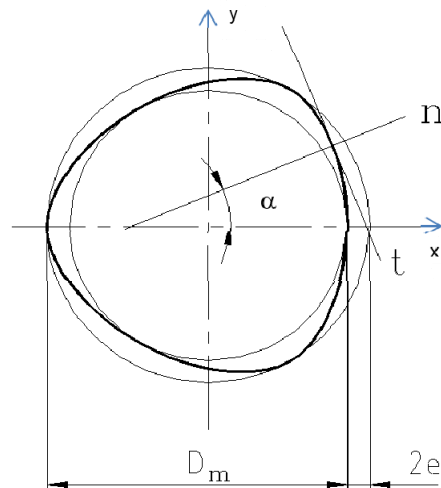
Figure 1: Polygonal profile with *n* = 3 lobes

$$x = \left[\frac{D_m}{2} - e \cdot \cos(n\alpha) \right] \cdot \cos\alpha - n \cdot e \cdot \sin(n\alpha) \cdot \sin\alpha$$

$$y = \left[\frac{D_m}{2} - e \cdot \cos(n\alpha) \right] \cdot \sin\alpha - n \cdot e \cdot \sin(n\alpha) \cdot \cos\alpha$$

(1)

In the preliminary stages of designing a new component, when many engineering solutions are considered, the use of FEM makes it difficult to quickly update a model subject to continuous shape optimisation. In these cases, it can be very advantageous to use BEM that performs the numerical study of a component by discretizing only the boundary, with the volume not being affected by the meshing operation and with a consequent reduction of "pre-processing" time. In addition, BEM, contrary to FEM, allows calculating traction and displacements at shaft-hub interface with the same accuracy (they are both *primary variables*). For this reason, it is highly suitable when studying problems with high surface stress gradients, such as contact problems.

In this paper a multi-objective optimization problem of a polygonal shaft-hub interference fit is analysed using the Taguchi method (robust design) [9-11], and the BEM commercial code BEASY [12].

BEM CONTACT STRESS ANALYSIS

Modelling of nonlinear contact [13] at shaft-hub interface takes place by means of special constraints ("normal gap"), defined between pair of nodes (*node to node contact*) belonging to overlapped elements at the interface area between the two zones (shaft and hub) in which the entire domain of the coupling is divided. Enforcing these constraints causes the code to consider the interface elements between the shaft and hub as separate, although initially coincident in modelling. Then a condition of interference or clearance is modelled, depending on the value, respectively negative or positive, attributed to the "normal gap".

The contact problems are nonlinear due to the variation of the contact area in dependence of the applied load. Therefore, the stress state at the interface depends on the friction coefficient, the load, the geometry as well as the material and extension of the contact area.

The nonlinear behaviour of the coupling was studied by means of an incremental-iterative procedure, which is useful when following the evolution of the contact as a result of the gradual application of the load, even in the presence of friction, which can be modelled in both static and dynamic terms [14].

It is worth highlighting the convenience of using an adequate number of regularly distributed (without circumferential "grading") linear elements rather than a smaller number of elements with higher polynomial order, on the interface area where the algorithm operates the contact. Such choice can improve the solution convergence and avoid "hot spots" occurrence (local irregularities at stress-deformational level in the numerical outcome).

The nature of the external applied load (torsional) requires for the remaining part of the surfaces a discretization with quadratic elements.
In the application that follows, an interference fit is assumed, with the global stresses resulting from the superposition of interference fit and torsional load.

PROBLEM DESCRIPTION

The problem relates to the optimal choice of the following design parameters of the coupling:
1. P3G profile of the coupling in terms of the eccentricity of the lobes (e);
2. type of lubricant interposed between the coupling surfaces, influencing the design friction coefficient (f);
3. coupling tolerances.

The objective is to minimize the effects of uncontrolled variability of the so called "noise factors" on the performance of the coupling while maximizing the performance parameters.
A DoE (Design of Experiments) approach was adopted, to define different configurations to be tested in the structural simulations, based on the use of so-called "orthogonal matrices". These simulations allow evaluating the performance parameters of the product, with particular reference to:
1. shaft-hub reciprocal circumferential sliding after loading, since limiting such sliding considerably increases the fatigue life of the joint;
2. maximum radial deformation of the hub, since excessive values could, for example, create malfunctioning if the hub is part of a kinematic chain (an alternative parameter may be the maximum error of circularity);
3. stress peaks in the hub (normally more stressed than the shaft), which must be limited in order to reduce its size and consequently the overall dimensions of the joint;
4. press fit force, since reduced values facilitate a possible isothermal assembly; this force ($F_{press\,fit}$) is evaluated as:

$$F_{press\,fit} = p_m * A * f$$

where p_m is the pressure at interface, assumed to be independent from the friction coefficient (f) and A is the contact surface.
It is also worth noting that the aforesaid mean pressure is just slightly influenced by the eccentricity value, depending substantially on the interference value.
Corresponding to the two profiles with $e=2.05mm$ and $e=3mm$, the perimeters are respectively $p_1=201\,mm$ and $p_2=207\,mm$.
The identified performance parameters should be limited as much as possible in absolute value (lower is better) but above all in terms of sensitivity to the varying "environmental" conditions (noise factors), so as to be able to predict with a reduced margin of uncertainty, the value that they will assume under operational conditions.
The noise factors, suitably simulated in each numerical analysis, are related to:
• the precision of the machining, which manifests itself through an interference fit value that is variable within the chosen tolerance zone;
• the variability of torque (torque peaks or overload in general);
• the variability of the friction coefficient compared to the nominal design value.
Finally, a series of numerical experiments L_4 (2^3) were carried out, based on three independent control variables and three noise factors, each with two possible levels.
In order to quantify the variability of the torque and the friction coefficient, a normal distribution was assumed, centred at the respective nominal values and with a variation coefficient σ/μ of nearly 7%. For the effective dimensions of shaft and hub the concept of "natural tolerance" was used, according to which the width of the tolerance zone is equal to 6σ and the mean value of the analysed dimension, which is also distributed according to a Gaussian function, is at the centre of the tolerance zone.
The adopted tolerance bands were IT7 (30 μm) for the hub and IT6 (19 μm) for the shaft and the corresponding standard deviations σ were equal to 30/6=5 μm and 19/6=3.17 μm respectively.
The normal distribution of the interferences (i) was obtained by composing the distributions of the size of the shaft (d_a) and hub (d_m) as follows:

$$i = d_a - d_m \quad \Rightarrow \quad \mu_i = \mu_{da} - \mu_{dm} \qquad \sigma_i^2 = \sigma_{da}^2 + \sigma_{dm}^2 = 25 + 10 = 35\ \mu m^2$$

Applying these formulas for the two considered couplings, the levels of the noise factors i_1 and i_2 were obtained, assuming that they are separated from each other by 2σ and are equidistant from the mean:

1. interference fit H7/n6 (i_{max}=39 µm; i_{min} = -10 µm; i_{med}=μ_i=14.5 µm; σ_i=5.9 µm):
   i_{11}= μ_i +σ_i=20.4 µm; $\quad$ i_{12}= μ_i -σ_i=8.6 µm;

2. interference fit H7/p6 (i_{max}=51 µm; i_{min}=2 µm; i_{med}=μ_i=26.5 µm; $\quad$ σ_i=5.9 µm):
   i_{21}= μ_i +σ_i = 32.4 µm; $\quad$ i_{22} = μ_i -σ_i=20.6 µm.

Regarding the applied torque, a nominal value M_t=1543 Nm was assumed (the chosen value does not affect the generality of the results). The values used in the simulation, again equidistant from the average value and each other distant 2σ, were M_{t1}=1651 Nm and M_{t2}=1442 Nm, with corresponding tractions on the external hub surface (Fig. 2) respectively equal to t_1=4.28 N/mm^2 and t_2=3.74 N/mm^2.

For the static friction coefficient that, as a control factor, was tested on two nominal levels f_1=0.2 and f_2=0.1, the corresponding levels of the noise factors were obtained with a variation of +/- 7% from such nominal values: f_{11}=0.214 and f_{12}=0.187, f_{21}=0.107 and f_{22}=0.0934, respectively. Together with the static friction coefficients, also the dynamic friction coefficients were provided as input to the analysis: the latter were assumed 20% lower than the static ones.

With reference to the geometry of the coupling, two different polygonal shaft-hub joints with three lobes were analysed: the first with eccentricity e=2.05 mm and the second with e=3 mm.

The trochoidal profile of the shaft was realised using the system Pro/ENGINEER (P.T.C.) [5] and imported into the calculation program through the IGES exchange format.

The BE analysis was initially carried out both with reference to the 3D (Fig. 2) and 2D models (Fig. 3), but for the sake of simplicity, the numerical experiments were carried out with reference to the 2D model. Under the action of a static torque, applied to the outer surface of the hub, the coupling exhibits a 120° cyclic symmetry; consequently, in order to reduce the computational effort, the analysis was carried out on just 1/3 of the entire model, imposing the boundary conditions of cyclic symmetry. One end of the shaft was assumed to be clamped whereas the torque M_t was introduced on the hub by means of tangential forces.
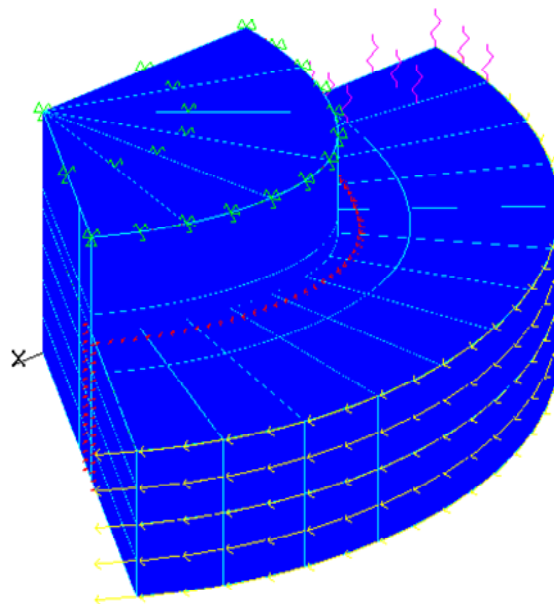

Figure 2: 3D polygonal coupling with highlight of boundary conditions.

The two models considered (A and B) had the following common dimensions (Figs. 1, 4): hub external diameter D_b=87 mm, diameter of the circle inscribed to the profile D_i=60 mm, hub length L_2=32.5 mm. The differences between the two models were related to:

- model A: e_A = 2.05 mm, D_m = 64.1 mm (Fig. 1);
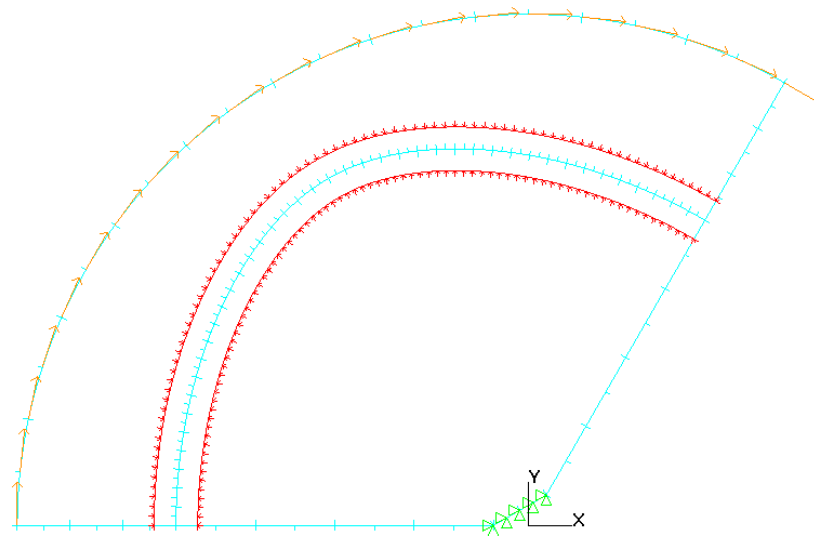- model B: e_B = 3 mm, D_m = 66 mm.

Figure 3: Mesh and boundary conditions of the coupling for the plane strain problem (symbols in red are representative of normal gap).
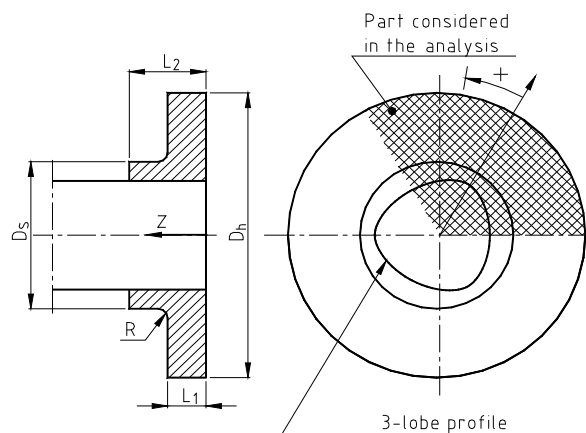

Figure 4: 3-lobe polygonal coupling parametric dimensions.

The shaft and hub were both made of steel (42CrMo4) with a Young's modulus E=216000 Nmm^{-2}, Poisson's ratio ν=0.3 and yield strength σ_s=800 Nmm^{-2}. The analysis was carried out under the hypothesis of isotropy, homogeneity and linear elasticity of the material.
In Fig. 5 a 2D example of the stress state induced by the combined action of the interference and torque is shown.

DESIGN OF EXPERIMENTS AND ANALYSIS OF THE RESULTS

The operating procedure requires the carrying out of several preliminary stages in order to design the experiments: identify the objective functions or performance parameters to be optimized; identify the control and noise factors and the related levels.
This phase involves the definition of the orthogonal matrix, which identifies the combinations of the control and noise factors relating to each simulation. For the design of numerical simulations, an orthogonal type L_4 (2^3) matrix was adopted

for both the control and noise factors. This matrix is suitable for the cases in question, since, in addition to providing a variation on two levels as required, it provides a number of simulations equal to the degrees of freedom and therefore just sufficient to ensure the conditions at the base of a correct use of the Taguchi method.
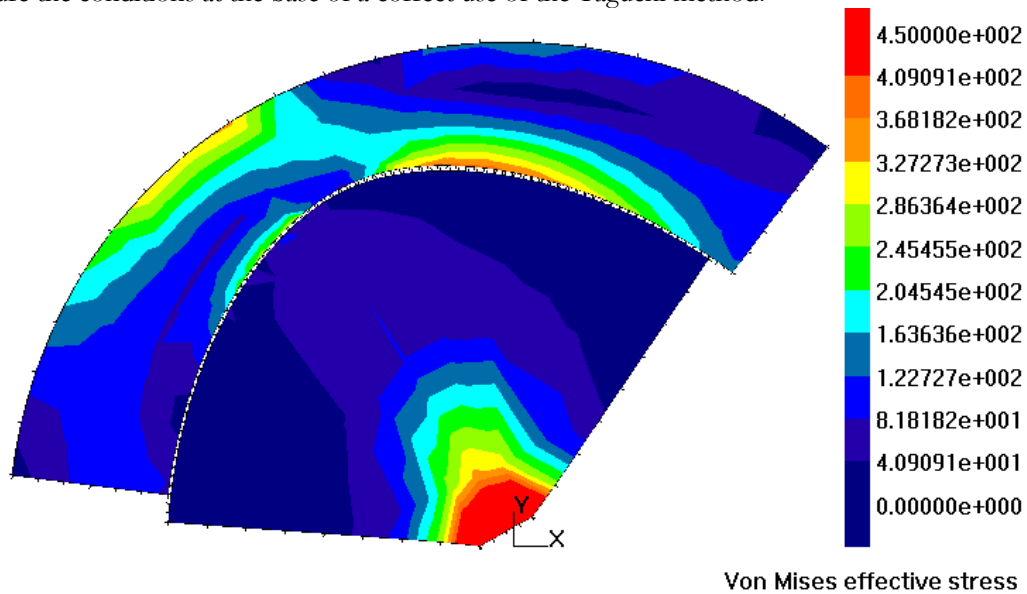

Von Mises effective stress

Figure 5: Von Mises stress (MPa) state induced by the combined action of interference and torque, with the highlight of circumferential reciprocal sliding.

Regarding the equivalent (Von Mises) stress peaks, it is worth considering the following:
- there is an optimal exploitation of the material when said peaks reach the maximum value allowed for the material in question, for which the problem is considered as *"nominal the best"*;
- the length of the hub can be chosen as calibration factor because useful in bringing the mean stress value to the target value after optimization, thanks to its characteristics (presumed but eventually verifiable) of not affecting the sensitivity of the coupling to considered noises. Thus, in the choice of the optimum combination of the design parameters, it is possible to neglect the distance between the target value and the effective mean value in the quality function. Only at the end the length of the hub is defined, upon which the stress peaks depend in an inversely proportional manner.

Figs. 6-10 show the effects of the control factors on the mean values and on the scatter of the performance parameters: with reference to the latter, each bar of the histogram is representative of the mean (Fig. 10) or the signal/noise ratio (Figs. 6-9), recalculated in decibels (dB), when the control factor, indicated on the abscissa, assumes a given value. Thus, the individual contributions of the control factors on the performance of the overall mean and S/N ratio are identified, assuming no interaction between the control factors. Tabs. 1-4 present all the simulation results.
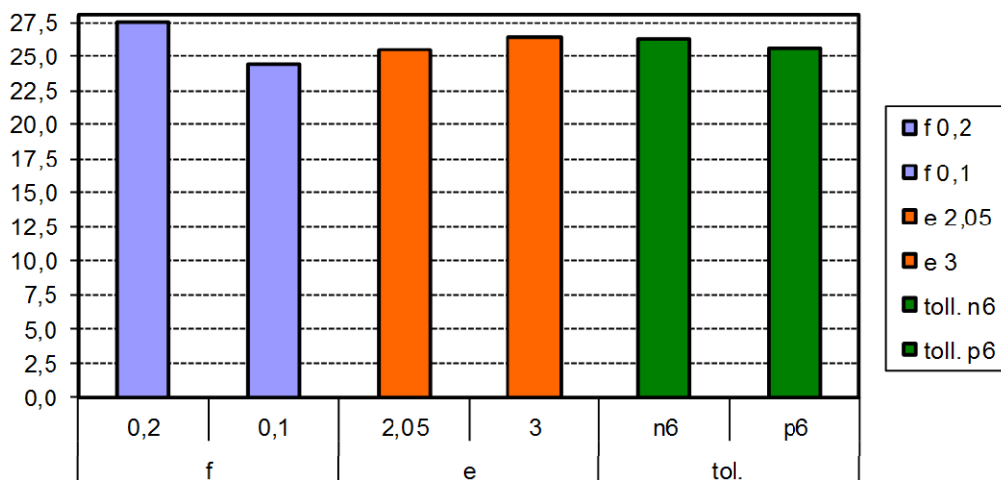

Figure 6: S/N ratio for the radial expansion of the hub upon varying the design parameters.
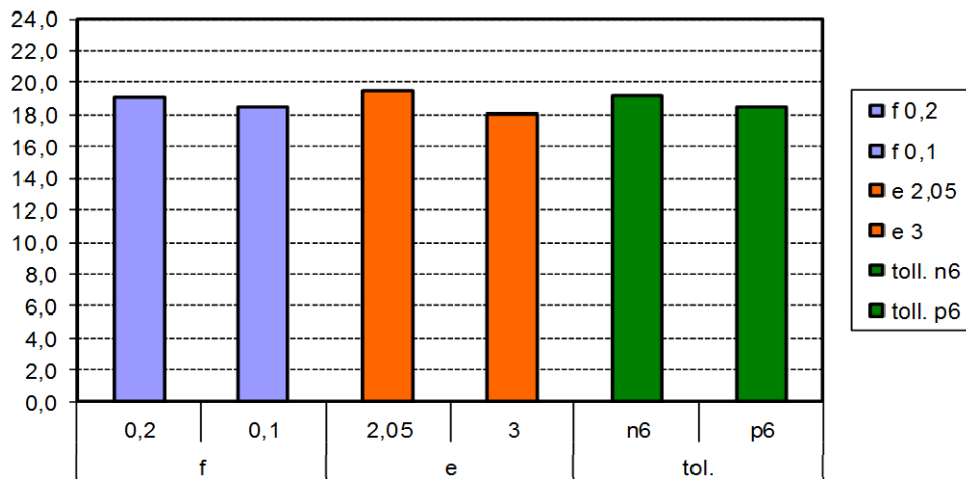
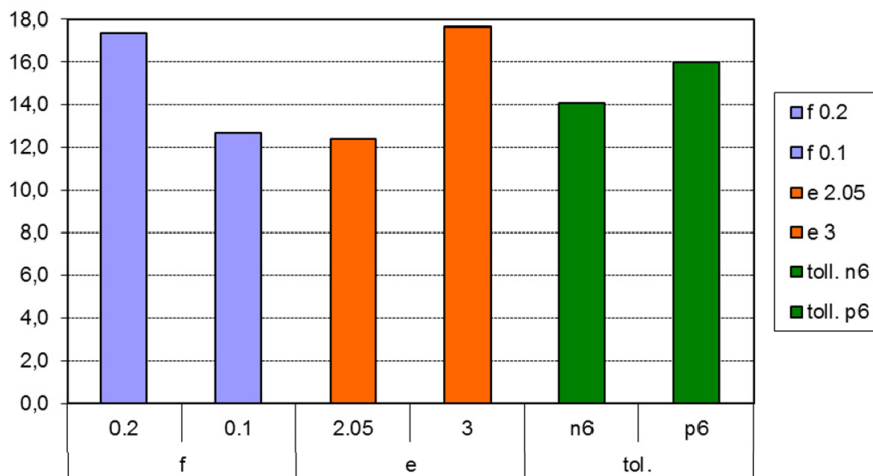Figure 7: S/N ratio for the Von Mises stress peaks in the hub upon varying the design parameters.

Figure 8: S/N ratio for the tangential shaft-hub displacements upon varying the design parameters.
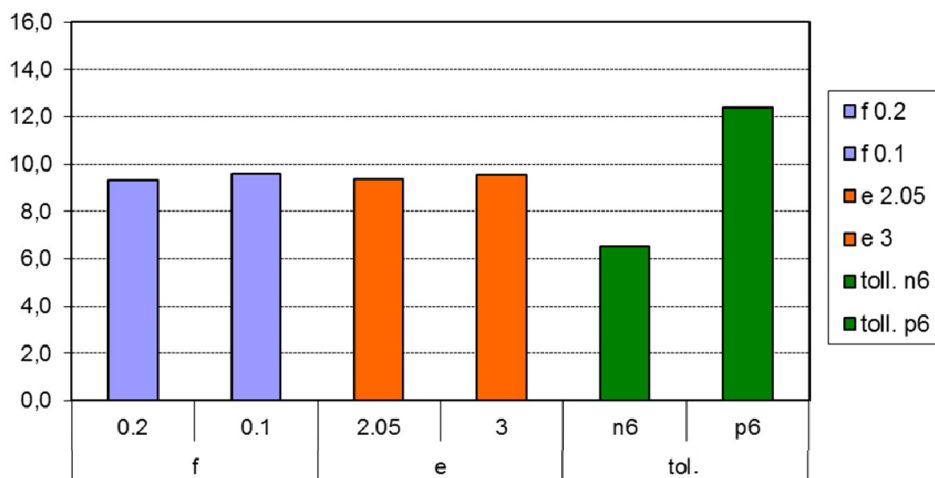

Figure 9: S/N ratio for the shaft-hub press fit force upon varying the design parameters.
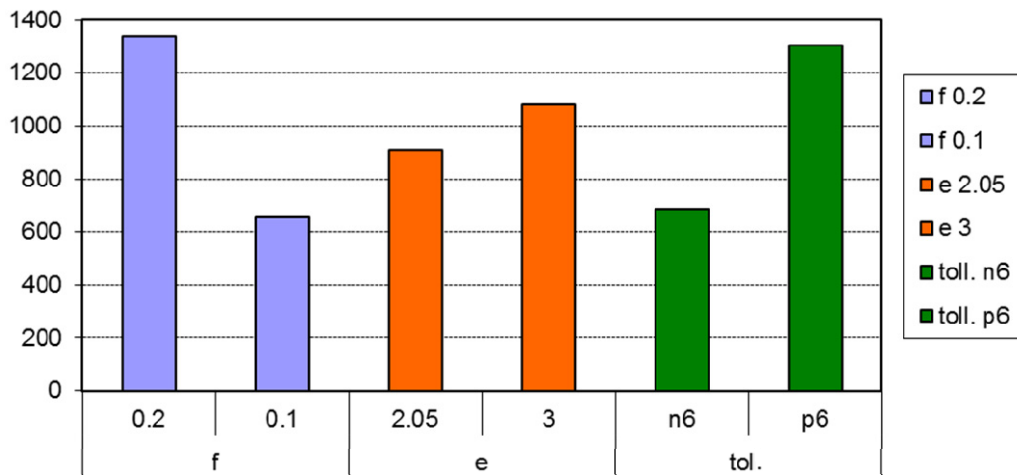
Figure 10: Mean values for the shaft-hub press fit force upon varying the design parameters.

Control factors (matrix L$_4$)			Noise factors (matrix L$_4$)				Average press fit force (N)	S/N ratio ($\eta=20Log_{10}(\mu/\sigma)$)
f	e	shaft tolerance grade	i1 f1 t1	i1 f2 t2	i2 f1 t2	i2 f2 t1		
0.2	2.1	n6	1419	1240	589	515	941	6.29E+00
0.2	3	p6	2215	1935	1484	1297	1733	1.23E+01
0.1	2.1	p6	1118	976	753	657	876	1.24E+01
0.1	3	n6	642	561	281	246	432	6.76E+00

Table 1: Average press fit force for an isothermal joint for each of the 16 tested configurations.

Control factors (matrix L$_4$)			Noise factors (matrix L$_4$)				Average equivalent stress value σ_{eq} (N/mm^2)	S/N ratio ($\eta=20Log_{10}(\mu/\sigma)$)
f	e	shaft tolerance grade	i1 f1 t1	i1 f2 t2	i2 f1 t2	i2 f2 t1		
0.2	2.05	n6	334	321	315	388	340	20.17
0.2	3	p6	552	543	417	477	497	17.93
0.1	2.05	p6	610	580	467	534	548	18.89
0.1	3	n6	550	500	405	480	484	18.10

Table 2: Von Mises stress peaks for each of the 16 tested configurations and relative sensitivity to noises.

Control factors (matrix L₄)			Noise factors (matrix L₄)				Average displacement (mm)	S/N ratio (η=-10Log₁₀(Σ(y$_i^2$)/n))
f	e	shaft tolerance grade	i1 f1 t1	i1 f2 t2	i2 f1 t2	i2 f2 t1		
0.2	2.05	n6	1.25E-01	1.15E-01	2.20E-01	3.00E-01	1.90E-01	1.38E+01
0.2	3	p6	8.10E-02	7.90E-02	7.90E-02	1.14E-01	8.83E-02	2.10E+01
0.1	2.05	p6	2.80E-01	2.52E-01	2.59E-01	3.30E-01	2.80E-01	1.10E+01
0.1	3	n6	1.78E-01	1.50E-01	1.90E-01	2.35E-01	1.88E-01	1.44E+01

Table 3: Maximum shaft-hub tangential displacements (mm) for each of the 16 tested configurations.

Control factors (matrix L₄)			Noise factors (matrix L₄)				Average hub radial expansion (mm)	S/N ratio (η=-10Log₁₀(Σ(y$_i^2$)/n))
f	e	shaft tolerance grade	i1 f1 t1	i1 f2 t2	i2 f1 t2	i2 f2 t1		
0.2	2.05	n6	3.60E-02	3.27E-02	4.38E-02	5.53E-02	4.20E-02	2.74E+01
0.2	3	p6	4.47E-02	4.45E-02	3.47E-02	4.26E-02	4.16E-02	2.76E+01
0.1	2.05	p6	7.01E-02	6.55E-02	5.84E-02	7.00E-02	6.60E-02	2.36E+01
0.1	3	n6	5.70E-02	5.05E-02	5.06E-02	6.10E-02	5.48E-02	2.52E+01

Table 4: Maximum hub radial expansion for each of the 16 tested configurations.

The identified optimal level assumes the following combination of the control factors:

• μ = 0.2 since it has a beneficial effect on all the performance parameters with the exception of the press fit force, which increases the mean value;

• *e* = 3 since, while slightly increasing the sensitivity of the stresses to the noises and the press fit force, it determines a beneficial effect on the relative displacements as well as on the radial expansion of the hub;

• interference fit H7/n6 since it reduces the stress state (it is worth recalling that stresses due to interference fit cannot be reduced by increasing the hub length), making it less sensitive to noises, even if the relative circumferential slidings increase, determining together with the eccentricity choice, a good compromise at the stress-strain level. This reduces the radial deformation of the hub as well as the press fit force that is already reduced by previous choices.

It is evident that if the priority of the designer were the fatigue life of the coupling rather than the static resistance, it would be better to choose the coupling H7/p6, which ensures a better tightening of the coupling, useful in preventing the phenomena of "fretting" (damage due to wear from relative motion under normal load).

CONFIRMATION EXPERIMENT TO VALIDATE THE PROCEDURE

At this point, it is possible to verify if the hypothesis of no interaction between the control factors are satisfied. This is achieved by the so-called confirmation experiment that simulates the behaviour of the joint in the identified optimal configuration by simultaneously superimposing noises. The obtained numerical results are then compared with those determined analytically to check their correspondence. If not verified, the assumptions made should be reviewed, resulting in the possible existence of interactions between the control factors or an incorrect setting of the objective functions. The optimum configuration is not present among those already simulated, with it being necessary to

carry out four additional simulations, corresponding to the four combinations of noise levels defined in the numerical plan. The performance parameters corresponding to the optimal configuration will come out from an average of the results obtained from the four simulations.

The confirmation experiment provided a positive assessment.

CONCLUSIONS

The adopted values of the control factors are varying in a small range since this analysis is part of a refinement that starts from a prior knowledge of the phenomenon and allows an a priori restriction of the domain in which to search for the optimum. This also explains the use of only two levels for the control and noise factors. The DoE approach allows to analyse a limited number of design configurations of the coupling without penalising the information content available from e.g. an extensive plan of numerical simulations, provided that there are no interactions (as in this case) between the control factors that would invalidate the applicability of the superposition principle.

BIBLIOGRAPHY

[1] Orlov, P., Fundamentals of Machine Design, MIR Publishers Moscow, 4 (1989) 69-73.
[2] Mechnik, R.P., Beitrag zur Festigkeitsberechnung von Polygon-Welle-Nabe-Verbindungen unter reiner Torsion, Konstruktion, 43 (1991).
[3] Strozzi, A., Baldini, A., Giacopini, M., Bertocchi, E., Bertocchi, L., Achievement of a uniform contact pressure in a shaft-hub press-fit, Proceedings of the Institution of Mechanical Engineers, Part C: Journal of Mechanical Engineering Science, 227(3) (2013) 405-419.
[4] Caputo, F., Giudice, G., Profili Poligonali per Trasmissione di Coppie: Analisi delle Tensioni e Verifica Sperimentale, In: Proceedings of the XII AIAS Conference, Sorrento, Italy, (1984).
[5] Citarella, R., Gerbino, S., BE analysis of shaft-hub couplings with polygonal profiles, Journal of Materials Processing Technology, 109 (2001) 30-37.
[6] Kollmann, F.G., Chr. Göttlicher, Entwicklung einer verbesserten Festigkeitsberechnung für P3G-Polygon-Welle-Nabe-Verbindungen beikombinierter Biege- und Torsionsbanspruchung, Zwischenber, DFG-Forsch. vorhaben Ko 634/34-1, TH-Darmastadt, (1992).
[7] Beitz, W., Reinholz, R., Tragfähigkeit von P3G-Welle-Nabe-Verbindungen, Konstr., 46 (1994).
[8] Filemon, E., Production and Analysis of Polygon Profiles, Periodica Polytechnica M III/1, Budapest, (1959).
[9] Taguchi, G., On Robust Technology Development, ASME Press, 1993
[10] Phadke, M. S. Quality Engineering Using Robust Design, Prentice Hall, Englewood Cliffs, NJ, USA, (1989).
[11] Park, S. H., Robust Design and Analysis for Quality Engineering, Chapman & Hall, 2-6 Boundary Row, London, (1996).
[12] BEASY V10r14, documentation, C.M. BEASY Ltd, (2011).
[13] Adey, R.A., Niku, S.M., Boundary element stress analysis involving contact using BEASY, In: Proc. Boundary Element Conference, Southampton, UK, (1999).
[14] Man, K.W., Aliabadi, M.H., Rooke, D.P., Analysis of Contact Friction using the Boundary Element Method, in Computational Methods in Contact Mechanics, M.H. Aliabadi and C.A. Brebbia, Eds, Computational Mechanics Publications, Southampton, Elsevier Applied Science, London, (1993) 1-60.